PHYSICAL REVIEW D **94,** 094037 (2016)

Aspects of the low-energy constants in the chiral Lagrangian for charmed mesons

Meng-Lin Du,[1,*] Feng-Kun Guo,[2,†] Ulf-G. Meißner,[1,3,‡] and De-Liang Yao[3,§]

[1]*Helmholtz-Institut für Strahlen- und Kernphysik and Bethe Center for Theoretical Physics, Universität Bonn, D–53115 Bonn, Germany*

[2]*CAS Key Laboratory of Theoretical Physics, Institute of Theoretical Physics, Chinese Academy of Sciences, Zhong Guan Cun East Street 55, Beijing 100190, China*

[3]*Institute for Advanced Simulation, Institut für Kernphysik and Jülich Center for Hadron Physics, Forschungszentrum Jülich, D-52425 Jülich, Germany*

(Received 14 October 2016; published 28 November 2016)

We investigate the numerical values of the low-energy constants in the chiral effective Lagrangian for the interactions between the charmed mesons and the lightest pseudoscalar mesons, the Goldstone bosons of the spontaneous breaking of chiral symmetry for QCD. This problem is tackled from two sides: estimates using the resonance-exchange model and positivity constraints from the general properties of the S-matrix including analyticity, crossing symmetry, and unitarity. These estimates and constraints are compared with the values determined from fits to lattice data of the scattering lengths. Tensions are found, and possible reasons are discussed. We conclude that more data from lattice calculations and experiments are necessary to fix these constants better. As a byproduct, we also estimate the coupling constant g_{DDa_2}, with a_2 the light tensor meson, via the QCD sum rule approach.

DOI: 10.1103/PhysRevD.94.094037

I. INTRODUCTION

Chiral perturbation theory (ChPT) [1–3], the low-energy effective field theory (EFT) of QCD, nowadays plays a crucial role in studying hadron physics at low energies. It is based on the spontaneous breaking of the approximate QCD chiral symmetry $\mathrm{SU}(N_f)_L \times \mathrm{SU}(N_f)_R$, where N_f is the number of light flavors, down to its vectorial subgroup $\mathrm{SU}(N_f)_V$. The lightest pseudoscalar mesons, much lighter than any other hadron, appear as the Goldstone bosons which are the effective degrees of freedom of ChPT. As a typical EFT, it accounts for the separation of energy scales in the physical systems under consideration: only the low-energy Goldstone modes are treated explicitly (external sources can be included easily), while the information of any other QCD excitation (at scales $\gtrsim \Lambda_\chi \sim 1$ GeV) is encoded in the coefficients in front of the local operators constructed from the Goldstone fields, which are unknown parameters and called low-energy constants (LECs) in ChPT. The determination of the chiral LECs is an important issue because it is essential for the predictive power of ChPT and further can serve as a consistency check of the theory.

Ideally, the LECs should be pinned down by comparing with (or performing fits to) experimental or lattice QCD data of selected observables in certain processes. Since these values of LECs should be universal, consequently, predictions for other processes or physical quantities can be made. For instance, the LECs of the fundamental πN interaction [4–9], which are fixed by fitting to experimental πN scattering data, are employed to make predictions in $\pi\pi N$ physics (see, e.g., Ref. [10]) and NN physics (see Ref. [11] for a review). However, things become cumbersome when there are not sufficiently many data or, even worse, no good data for fixing the LECs. Furthermore, even if the LECs have been extracted or estimated using some procedure, the reliability of these values still needs to be further analyzed.

A phenomenological approach to estimate the LECs was discussed in detail in Refs. [12–14] and is traditionally referred to as the resonance saturation. Therein, phenomenological Lagrangians respecting chiral symmetry including explicit meson resonances are constructed, and then the resonance fields are integrated out to generate contributions to the LECs in the mesonic ChPT Lagrangian at tree level in terms of the resonance couplings and masses. It was found that whenever the vector and axial vector mesons contribute they almost saturate the empirical values of the LECs, which is a modern version of the vector meson dominance hypothesis. Similarly, the resonance-exchange model also provides a fairly good phenomenological description of the LECs in the chiral Lagrangian for the pion-nucleon interactions, cf. Ref. [15], where it is found that the Δ resonance provides the dominant contribution to some of the LECs, i.e., c_3 and c_4.[1] In view of

*du@hiskp.uni-bonn.de
†fkguo@itp.ac.cn
‡meissner@hiskp.uni-bonn.de
§d.yao@fz-juelich.de

[1]Note that there is also an important contribution from the ρ meson to c_4.

the success achieved in both the purely mesonic ChPT and baryon ChPT, the resonance-exchange method will be discussed in this paper to estimate the LECs related to the interactions between charmed D mesons and Goldstone bosons (to be denoted as ϕ), which are badly known because no experimental data for $D\phi$ scattering are available and almost all the existing extractions result from fitting to lattice results of scattering lengths for certain channels.

The $D\phi$ interaction is of great importance in understanding the heavy-light meson spectrum on the one hand and serves as an ideal playground to combine heavy-quark symmetry (HQS) and chiral symmetry on the other one. A good example for the former is provided by the $D_{s0}^*(2317)$ discovered in 2003 [16,17]. As this state might be a DK bound state [18], progress toward unravelling its nature has been made along the line of studying the interaction between the D meson and the kaon [19–27].

The $D\phi$ interaction can also give guidance for $D^*\phi$, $B\phi$, and $B^*\phi$ interactions, since similarities among them exist due to heavy-quark spin and flavor symmetries [28–30]. The heavy-quark symmetries relate the pseudoscalar D mesons to the vector D^* as well as to the bottom analogs. Thus, the LECs determined in one sector can be used in the other heavy-quark-symmetry-related sectors at leading order of the heavy-quark expansion once the heavy-quark mass scaling is properly taken into account.

Partly stimulated by the lattice QCD results for the $D\phi$ scattering lengths in the past few years [25,26,31,32], the $D\phi$ interaction has been revisited using the chiral Lagrangian up to the next-to-leading order (NLO) or the next-to-next-to-leading order (NNLO), and the LECs are determined from fitting to the lattice results of the scattering lengths using either perturbative [33,34] or unitarized scattering amplitudes [25,35–38]. However, the scarcity of data and the model dependence of the unitarization method cause discrepancies among the extracted values for some of the LECs.

Furthermore, we will investigate model-independent positivity constraints on the $D\phi$ interaction as well. Similar to the case for the $\pi\pi$ [39–43] and πN [44,45] scattering, these constraints will be derived in the upper part of the Mandelstam triangle (with $t > 0$) based on axiomatic principles of the S-matrix theory such as analyticity, unitarity, and crossing symmetry. After applying the obtained constraints to the chiral perturbative and extended-on-mass shell (EOMS) renormalized amplitudes, e.g., given by Ref. [37], one obtains restrictions on the involved LECs at a certain given order. These axiomatic constraints will be confronted with the numerical values of the LECs determined through various phenomenological fits to lattice data.

This paper is structured as follows. In Sec. II A, we start with a brief review of the formal aspects of $D\phi$ scattering. In Sec. II B, we discuss the possible resonances that should be taken into consideration and introduce the relevant phenomenological Lagrangians for resonance exchange. Then, in Sec. II C, we compute the resonance contributions to the LECs at tree-level analytically and numerically. In Sec. III, we deal with the axiomatic constraints on the $D\phi$ scattering amplitudes in perturbation theory, which are finally transformed into positivity bounds on the LECs, and we will compare these constraints with the determinations in nonperturbative fits to lattice data. A summary of this work is given in Sec. IV. The leading order (LO) Born-term contributions to $D\phi$ scattering are relegated to Appendix A for completeness. We collect the contribution to LECs from the exchange of light tensor mesons and an estimate of their coupling to the D-meson g_{DDT} using the QCD sum rule approach in the Appendixes B and C, respectively.

II. LOW-ENERGY CONSTANTS AND RESONANCE EXCHANGES

In this section, we give a short introduction to some relevant issues related to $D\phi$ scattering, such as the involved LECs and the related Mandelstam plane. Then, the LO chiral Lagrangians for various resonances are discussed and constructed for later use. Finally, we make use of the approach of resonance exchange to analyze the resonance contributions to the LECs. The corresponding numerical results are also given.

A. $D\phi$ scattering at low energies

As mentioned in the Introduction, the pseudoscalar and vector charmed mesons are related to each other via heavy-quark spin symmetry. One can construct ChPT for heavy mesons by treating the pseudoscalars and the vectors simultaneously in a spin multiplet. The scattering processes of the Goldstone bosons off the pseudoscalar and vector charmed mesons can thus be described by the same chiral Lagrangian at low energies. The LECs of such a Lagrangian will be discussed in this paper. So far, most of the available information for these LECs was obtained from fitting to the lattice data of the S-wave scattering lengths for the $D\phi$ systems [25,37]. It has been shown by explicit calculations that the D^* contribution is negligible in these quantities [37,46]. Hence, we can focus on the Lagrangian without the D^* and keep in mind that such a theory is basically equivalent to the one with the D^* explicitly included when discussing the S-wave $D\phi$ scattering. The relevant chiral effective Lagrangian reads [25,37][2]

[2]There are in fact four more terms at $\mathcal{O}(p^3)$ which can be found in Ref. [47]. However, they do not contribute to the $D\phi$ scattering and thus will not be discussed here.

$$\mathcal{L}_{D\phi} = \mathcal{D}_\mu D \mathcal{D}^\mu D^\dagger - \mathring{M}^2 D D^\dagger + D(-h_0\langle\chi_+\rangle - h_1\chi_+ + h_2\langle u_\mu u^\mu\rangle - h_3 u_\mu u^\mu)D^\dagger + \mathcal{D}_\mu D(h_4\langle u_\mu u^\nu\rangle - h_5\{u^\mu, u^\nu\})\mathcal{D}_\nu D^\dagger + D[ig_1[\chi_-, u_\nu] + g_2([u_\mu, [\mathcal{D}_\nu, u^\mu]] + [u_\mu, [\mathcal{D}^\mu, u_\nu]])]\mathcal{D}^\nu D^\dagger + g_3 D[u_\mu, [\mathcal{D}_\nu, u_\rho]]\mathcal{D}^{\mu\nu\rho} D^\dagger + \text{higher-order terms}, \quad (1)$$

where the building blocks are given by

$$u_\mu = i(u^\dagger\partial_\mu u - u\partial_\mu u^\dagger), \qquad \chi_\pm = u^\dagger\chi u^\dagger \pm u\chi^\dagger u, \quad (2)$$

with $\chi = 2B_0\text{diag}(m_u, m_d, m_s)$ and

$$u = \exp\left(\frac{i\phi}{\sqrt{2}F_0}\right), \qquad \phi = \begin{pmatrix} \frac{1}{\sqrt{2}}\pi^0 + \frac{1}{\sqrt{6}}\eta & \pi^+ & K^+ \\ \pi^- & -\frac{1}{\sqrt{2}}\pi^0 + \frac{1}{\sqrt{6}}\eta & K^0 \\ K^- & \overline{K}^0 & -\frac{2}{\sqrt{6}}\eta \end{pmatrix}. \quad (3)$$

Here, B_0 is a constant related to the quark condensate. F_0 and $\mathring{M}$ are the pion decay constant and the mass of pseudoscalar charmed mesons in the chiral limit, respectively. The coupling constants h_i, g_i are the LECs to be discussed in this paper. D denotes the SU(3) triplet of the ground-state pseudoscalar charmed mesons, i.e., $D = (D^0, D^+, D_s^+)$. $\mathcal{D}_\mu$ is the chirally covariant derivative acting on the D-meson fields, and $\mathcal{D}^{\mu\nu\rho} = \{\mathcal{D}_\mu, \{\mathcal{D}_\nu, \mathcal{D}_\rho\}\}$.

It is worth noting that the mass dimensions of the LECs $h_{i=0,\ldots,5}$ as defined in Refs. [25,37] are different, so are those for $g_{j=1,2,3}$. Therefore, in Refs. [25,37], the following redefinitions of the LECs are employed,

$$h'_{4,5} = h_{4,5}\overline{M}_D^2, \quad h_{24} = h_2 + h'_4, \quad h_{35} = h_3 + 2h'_5, \quad g_{23} = g'_2 - 2g'_3, \quad g'_{1,2} = g_{1,2}\overline{M}_D, \quad g'_3 = g_3\overline{M}_D^3, \quad (4)$$

where $\overline{M}_D = (M_D^{\text{phy}} + M_{D_s}^{\text{phy}})/2$, with M_D^{phy} and $M_{D_s}^{\text{phy}}$ the physical masses of the D and D_s mesons, respectively. These newly defined coefficients of the $\mathcal{O}(p^2)$ and $\mathcal{O}(p^3)$ operators are in units of 1 and GeV^{-1}, respectively. The $h_{0,1}$ are dimensionless, too. As discussed in Ref. [25], such redefinitions are also designed to reduce the correlations between the LECs and are useful and necessary to obtain reliable numeral results when performing fits.

For $D\phi$ scattering, there are in total 16 channels with different strangeness S and isospin I quantum numbers. Nevertheless, since the scattering amplitudes $\mathcal{A}(s,t)$ are related to each other according by crossing symmetry, only ten amplitudes are independent in the end and can be taken as the basis to construct the other amplitudes. The ten amplitudes calculated in the physical particle bases following Refs. [24,37] are given in Appendix A. They will be used when deriving the resonance-exchange amplitudes in Sec. II C.

Before ending this subsection, let us introduce the Mandelstam plane which will be used when deriving the positivity constraints. In the Mandelstam s–t plane, the kinematical region of the $D\phi$ scattering is defined as the domain where the Kibble function [48] $\Phi = t[su - (M_D^2 - M_\phi^2)^2]$ is non-negative. The plane is depicted in Fig. 1, where the bottom-right, bottom-left, and top areas in light gray denote the s-, u-, and t-channel physical regions, respectively. The interior of the triangle surrounded by lines of $s = (M_D + M_\phi)^2$, $u = (M_D + M_\phi)^2$, and $t = 4M_\phi^2$ is called the Mandelstam triangle, where the scattering amplitude is real and analytical. The positivity constraints will be calculated in the upper part of the Mandelstam triangle where $t \geq 0$; see the area marked in dark gray in Fig. 1. Notice that the condition $t \geq 0$ guarantees that the Legendre polynomials $P_\ell(\cos\theta)$, with θ the scattering angle, are non-negative, which is necessary for deriving the positivity constraints [41,42,45].

B. Chiral resonance Lagrangians

The saturation of LECs by the contributions from resonances is based on scale separation such that the low-energy effective Lagrangian contains only the low-lying degrees of freedom and the resonances at the hard scale are considered to be integrated out. The local operators in the Lagrangian are constructed in terms of the effective degrees of freedom, while the high-energy contribution including the effects from resonances enter the LECs, which are coefficients of the operators. In principle, the LECs can be calculated in the full theory by a matching procedure. In the case of the chiral Lagrangian, since we cannot solve the nonperturbative QCD analytically, we may match the chiral Lagrangian containing only the low-lying degrees of freedom to the one with resonances, which is applicable in a larger energy range phenomenologically despite the more complicated renormalization and power-counting issues related to the large masses and instability of the resonances. For such a matching, one expects that the resonances with relatively low masses contribute dominantly to the LECs.

To analyze the resonance contributions to the chiral LECs, the chiral resonance Lagrangians are necessary. We will first introduce the Lagrangians related to excited

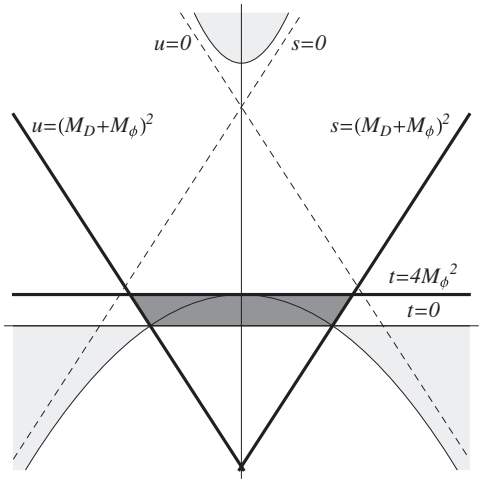

FIG. 1. The Mandelstam plane. The Mandelstam triangle is the region bounded by the thick lines: $s = (M_D + M_\phi)^2$, $u = (M_D + M_\phi)^2$, and $t = 4M_\phi^2$. The upper part of the Mandelstam triangle is marked in dark gray, which is surrounded by the previous three lines and the one corresponding to $t = 0$. The physical regions are marked in light gray.

charmed mesons, with the orbital angular momentum between the charmed quark and light quark $\ell \leq 1$, and then the ones concerning the light-flavor mesonic excitations will be discussed.

The excited charmed mesons with $\ell \leq 1$ include D_0^* with $J^P = 0^+$, D_1' and D_1 with $J^P = 1^+$, and D_2^* with $J^P = 2^+$.[3] Though more and more candidates for states with $\ell \geq 2$ were discovered experimentally [49–51], their classifications in the charmed spectra still need to be investigated or confirmed. Furthermore, their contributions should be smaller than those with $\ell \leq 1$ because of higher masses as mentioned above. Hence, we do not include them in our analysis.

For the scalar D_0^* SU(3) triplet, $D_0^* = (D_0^{*0}, D_0^{*+}, D_{s0}^{*+})$, the corresponding Lagrangian is

$$\mathcal{L}_{D_0^* D\phi} = g_0 (D_0^* u^\mu \mathcal{D}_\mu D^\dagger + \mathcal{D}_\mu D u^\mu D_0^{*\dagger}). \tag{5}$$

The coupling g_0 will be determined via the LO calculation of the decay $D_0^* \to D^+ \pi^-$.

As for the tensor D_2^* triplet, $D_2^* = (D_2^{*0}, D_2^{*+}, D_{s2}^{*+})$, the lowest-order Lagrangian for the $D_2^* D\phi$ interaction,

$$\mathcal{L}_{D_2^* D\phi} \propto D_{2,\mu\nu}^* \{\mathcal{D}^\mu, u^\nu\} D^\dagger + \text{H.c.}, \tag{6}$$

is of second chiral order. Physically, the coupling of a tensor charmed meson to a pseudoscalar charmed meson and a light pseudoscalar is in a D wave and starts from $\mathcal{O}(p^2)$. Thus, the exchange of tensor charmed mesons will not contribute to the LECs in the $\mathcal{O}(p^2)$ and $\mathcal{O}(p^3)$ Lagrangians, and its contribution starts from $\mathcal{O}(p^4)$ in the chiral expansion.

[3]Note that the D^* vector mesons with $J^P = 1^-$ are treated as the spin partner of the D as discussed at the beginning of this section.

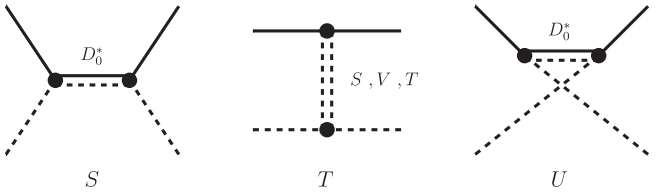

FIG. 2. Diagrams for the resonance-exchange contribution to $D\phi$ scattering.

The axial vector charmed mesons D_1 and D_1' do not contribute to the LECs in the chiral Lagrangian for the $D\phi$ interactions since there is no $D_1^{(\prime)} D\phi$ coupling due to parity conservation. Yet, they will contribute to those in the $D^*\phi$ Lagrangian. At leading order of the heavy-quark expansion, such contributions are equal to those of the D_0^* and D_2^* to the $D\phi$ Lagrangian.

Therefore, among the excited charmed mesons, we only need to take into account the exchange of the scalar ones for our purpose of estimating resonance contributions to the $\mathcal{O}(p^2)$ and $\mathcal{O}(p^3)$ LECs. With the above Lagrangians, we can then calculate the $D\phi$ scattering amplitudes by exchanging the D_0^* of which the Feynman diagrams are shown in Fig. 2 (see the first and third diagrams). It is evident that they contribute to $D\phi$ scattering in both the s and u channels.

For the light-flavor mesonic resonances, the low-lying vector, scalar, and tensor states will be considered. They contribute to $D\phi$ scattering in the t channel; see the second Feynman diagram in Fig. 2. For the vector resonance, the involved interactions read [12,13]

$$\begin{aligned} \mathcal{L}_{V\phi\phi} &= \frac{ig_V}{\sqrt{2}} \langle \hat{V}_{\mu\nu} u^\mu u^\nu \rangle, \qquad (\hat{V}_{\mu\nu} \equiv \partial_\mu V_\nu - \partial_\nu V_\mu), \\ \mathcal{L}_{DDV} &= ig_{DDV} \{ D V^\mu (\partial_\mu D^\dagger) - (\partial_\mu D) V^\mu D^\dagger \}, \end{aligned} \tag{7}$$

where V_μ denotes the vector meson multiplet of interest with its explicit form given by

$$V_\mu = \begin{pmatrix} \frac{\rho^0}{\sqrt{2}} + \frac{\omega}{\sqrt{2}} & \rho^+ & K^{*+} \\ \rho^- & -\frac{\rho^0}{\sqrt{2}} + \frac{\omega}{\sqrt{2}} & K^{*0} \\ K^{*-} & \overline{K}^{*0} & \tilde{\phi} \end{pmatrix}_\mu . \tag{8}$$

Here, the ideal mixing scheme between ω_1 and ω_8, i.e., $\omega_1 = \sqrt{2/3}\omega + \sqrt{1/3}\tilde{\phi}$ and $\omega_8 = \sqrt{1/3}\omega - \sqrt{2/3}\tilde{\phi}$, is employed to construct the physical ω and $\tilde{\phi}$. Note that we have denoted the physical $\phi(1020)$ by the symbol $\tilde{\phi}$ in

order to avoid possible confusion with the notation for the matrix of Goldstone bosons.

The Lagrangians concerning the scalar resonance exchange take the form [12,13]

$$\mathcal{L}_{S\phi\phi} = c_d\langle S u_\mu u^\mu\rangle + c_m\langle S\chi_+\rangle + \tilde{c}_d S_1\langle u_\mu u^\mu\rangle + \tilde{c}_m S_1\langle\chi_+\rangle,$$
$$\mathcal{L}_{DDS} = g_{DDS} DSD^\dagger + \tilde{g}_{DDS} DD^\dagger S_1, \tag{9}$$

with S_1 and S denoting the scalar singlet and octet, respectively. In Eqs. (7) and (9), the Lagrangians for the coupling of the light-flavor resonances to the Goldstone bosons are taken from Refs. [12,13].

Finally, we also consider the light-flavor tensor resonances with quantum numbers 2^{++}. We collect the corresponding Lagrangians and the contribution to LECs in Appendix B. The involved coupling between the D mesons and the tensor resonance, g_{DDT}, is estimated via the method of QCD sum rules in Appendix C.

C. Resonance contributions to the LECs

The resonance-exchange amplitudes, corresponding to the Feynman diagrams in Fig. 2, are calculated, and their explicit expressions are given in Appendix A for completeness.[4] To calculate the tree-level resonance-exchange contribution to the LECs, these Born-term amplitudes are expanded in terms of $s - M_0^2$, M_ϕ^2, and t and then compared with the contact term contributions given in Ref. [37]. Consequently, the D_0^*-exchange contributions to the LECs are

$$h_5^{D_0^*} = -\frac{g_0^2}{2\Delta_0^2},$$
$$g_1^{D_0^*} = g_2^{D_0^*} = g_3^{D_0^*}\Delta_0^2 = -\frac{g_0^2}{8\Delta_0^2}, \tag{10}$$

with the difference of the squared masses, $\Delta_0^2 \equiv \mathring{M}_0^{*2} - \mathring{M}_0^2$, where $\mathring{M}_0^*$ is the chiral limit mass of the D_0^*.

The light vector mesons contribute to g_1 and g_2 as follows:

$$g_1^V = g_2^V = -\frac{g_{DDV} g_V}{2\sqrt{2} M_V^2}. \tag{11}$$

From the above equations, we note that light vector-meson exchange does not contribute to any LEC in the $\mathcal{O}(p^2)$ Lagrangian, which is different from the pion-nucleon case in Ref. [15]. This is due to the fact that the Lorentz index of the vector is contracted with the Gamma matrices in the nucleon case, but in our case with those of the derivatives of the D mesons. For a t-channel exchange, this partial derivative contributes as $\mathcal{O}(p^1)$. Together with the $\mathcal{O}(p^2)$ $V\phi\phi$ vertex, the t-channel vector-meson exchange thus starts to contribute at $\mathcal{O}(p^3)$.

The light-flavor scalar mesons contribute as

$$h_0^S = -\frac{\tilde{g}_{DDS}\tilde{c}_m}{M_{S1}^2} + \frac{g_{DDS}c_m}{3M_{S8}^2}, \qquad h_1^S = -\frac{g_{DDS}c_m}{M_{S8}^2},$$
$$h_2^S = \frac{\tilde{g}_{DDS}\tilde{c}_d}{M_{S1}^2} - \frac{g_{DDS}c_d}{3M_{S8}^2}, \qquad h_3^S = -\frac{g_{DDS}c_d}{M_{S8}^2}. \tag{12}$$

Here, M_{S1} and M_{S8} denote the masses of singlet and octet scalars, respectively. Without entering the discussion about which values should be used for the light scalar multiplets, we make use of large N_c and set $M_S = M_{S_1} = M_{S_8}$, as done in Ref. [15]. Furthermore, the singlet couplings can be expressed in terms of the octet ones through the relations: $\tilde{c}_{m,d} = c_{m,d}/\sqrt{3}$ and $\tilde{g}_{DDS} = g_{DDS}/\sqrt{3}$. By imposing these large-N_c relations, the above expressions in Eqs. (12) are reduced to

$$h_0^S = 0, \qquad h_1^S = -\frac{g_{DDS}c_m}{M_S^2},$$
$$h_2^S = 0, \qquad h_3^S = -\frac{g_{DDS}c_d}{M_S^2}. \tag{13}$$

One sees that the LECs h_0 and h_2 receive no contribution from the light scalar mesons in the large-N_c limit. In fact, these two LECs, together with h_4, are of one order higher in the $1/N_c$ expansion in comparison with $h_i (i = 1, 3, 5)$ [23,52].

As shown in Appendix B, the exchange of light tensor mesons with $J^{PC} = 2^{++}$ contributes only to h_5, which is of the form

$$h_5^T = \frac{g_{DDT} g_T}{M_T^2}, \tag{14}$$

with g_{DDT} and g_T the coupling constants for $D - D$-tensor and $\pi - \pi$-tensor vertices, respectively; see Eqs. (B1) and (B4). This contribution was calculated by employing the technique used in Refs. [12,13], namely, matching the effective actions, which is equivalent to the approach we have used above that is based on the matching using the explicit perturbative amplitudes in both theories.

D. Numerical results

To obtain numerical estimates for the LECs, we need to know the resonance couplings. However, not all of the involved couplings are really known. Thus, for the measurable ones ($\tilde{g}$, g_0, g_V, c_d, c_m, and g_T), we will extract the values from experimental data, and for the ones in the vertices where not all three particles can go on shell

[4] In Appendix B, we will employ the technique used in Refs. [12,13] to calculate the contribution of light tensor resonances, which is different from the one used here.

simultaneously (g_{DDV}, g_{DDS}, and g_{DDT}), we will take model values for an estimate.

The numerical value of the resonance coupling g_0 can be obtained by calculating the decay width $\Gamma(D_0^* \to D^+\pi^-)$. At LO, we have

$$\Gamma(D_0^* \to D^+\pi^-) = \frac{1}{4\pi}\frac{|g_0^2|}{F_0^2}\frac{(M_{D_0^*}\sqrt{M_\pi^2 + |\vec{q}_\pi|^2} - M_\pi^2)^2}{M_{D_0^*}^2}, \tag{15}$$

with $\vec{q}_\pi$ the pion momentum in the rest frame of the initial particle. Comparing with the empirical value taken from the Particle Data Group [53], we get

$$|g_0| = 0.68 \pm 0.05. \tag{16}$$

The couplings of the light-flavor resonances to the Goldstone bosons, g_V and $c_{m,d}$, have been used in many studies of the chiral resonance Lagrangian, and we take the updated determinations in Ref. [54]:

$$|g_V| = 0.0846 \pm 0.0008, \qquad |c_m| = (80 \pm 21)\ \text{MeV},$$
$$|c_d| = (26 \pm 7)\ \text{MeV}. \tag{17}$$

From the decay width of the $f_2(1270) \to \pi\pi$ [53], we get $|g_T| = 28$ MeV. Note that, as discussed in Ref. [15], if the πN LEC c_1 is completely saturated by scalar exchange, a positive c_m is demanded. Together with the constraint $4c_m c_d = F_0^2$, see, e.g., Ref. [55], we will set $c_{m,d} > 0$ in the following.

For the troublesome couplings, we take the following values:

$$g_{DDV} = 1.46, \qquad g_{DDS} = 5058\ \text{MeV},$$
$$g_{DDT} = 3.9 \times 10^{-3}\ \text{MeV}^{-1}. \tag{18}$$

The value of g_{DDV} is taken from the analysis of the DDV vertex using light-cone QCD sum rules [56]. For the g_{DDS}, we have utilized the large-N_c relation $g_{DDS} = \sqrt{3}\tilde{g}_{DDS}$ and take the value $g_{DD\sigma}$ used in Ref. [57], which was extracted from the parity doubling model of Ref. [58], for $\tilde{g}_{DDS}$. There is no available modeling of g_{DDT}, and we thus estimate it using QCD sum rules in Appendix C. The problem is that it is hard to quantify the uncertainty of these parameters. Yet, there is evidence that these model values are of the right order: the dimensionless values for g_{DDV}, $g_{DDS}/\Lambda_{\text{had}} \sim 5$, and $g_{DDT}\Lambda_{\text{had}} \sim 4$, where $\Lambda_{\text{had}} = \mathcal{O}(1\ \text{GeV})$ is a typical hadronic scale, have more or less natural sizes of $\mathcal{O}(1)$.

For the masses involved in our numerical estimate, we take

TABLE I. Estimates of the resonance contributions to the LECs. Here, $h_{0,2,4}$, which vanish in the large-N_c limit, are not shown. The columns starting with D_0^*, V, S, and T list the contributions from the exchange of the scalar charmed mesons, light-flavor vector, scalar, and tensor mesons, respectively. The last column sums over all these contributions.

LEC	D_0^*	V	S	T	Total
h_1	0	0	0.4	0	0.4
h_3	0	0	0.1	0	0.1
h_5 (GeV^{-2})	-0.1	0	0	± 0.1	$[-0.2, 0.0]$
g_1 (GeV^{-2})	-0.03	∓ 0.07	0	0	$[-0.1, 0.04]$
g_2 (GeV^{-2})	-0.03	∓ 0.07	0	0	$[-0.1, 0.04]$
g_3 (GeV^{-4})	0.02	0	0	0	0.02

$$\mathring{M} \cong \overline{M}_D = \frac{1}{2}(M_D^{\text{phy}} + M_{D_s}^{\text{phy}}) = 1918\ \text{MeV},$$
$$\mathring{M}_0^* \cong \overline{M}_{D_0^*} = \frac{1}{2}(M_{D_0^*}^{\text{phy}} + M_{D_{s0}^*}^{\text{phy}}) = 2318\ \text{MeV},$$
$$M_V = 764\ \text{MeV}, \qquad M_S = 980\ \text{MeV},$$
$$M_T = 1270\ \text{MeV}, \tag{19}$$

where the chiral limit masses are identified with the corresponding averaged physical masses, which is acceptable given the accuracy we are aiming at. To be consistent with using the values of g_V and $c_{m,d}$ given above, the values for M_V and M_S are also taken from Ref. [54]. The mass for the tensor multiplet is chosen to be the mass of $f_2(1270)$ following Ref. [59].

With the resonance couplings and masses specified above, we are now in the position to estimate the resonance contributions to the LECs based on the analytical expressions, Eqs. (10)–(14). The numerical results are shown in Table I, and the sum of various contributions is given in the last column. Because of the poor knowledge on the values of the off-shell couplings $g_{DDV,DDS,DDT}$, no reasonable error estimate can be made here. Furthermore, the signs of $g_{V,T}$ are not fixed, and hence contributions from the t-channel exchanges of the light-flavor vector and tensor mesons might be either positive or negative as listed in Table I, and they also take two possible values in the last column of the table due to interference with the contribution from the scalar charmed mesons.

E. Comparison with results from unitarized ChPT

We compare the estimates of the LECs with those from fits to the lattice data on scattering lengths of some selected channels at the NLO and NNLO in the framework of unitarized (UChPT) [60] (and references therein) in Tables II and III, respectively, where the definitions of

TABLE II. Comparison of the values of the LECs from the estimate using resonances with those from fits to lattice data in various formulations of unitarized ChPT at NLO. The LECs in this table are dimensionless.

LEC	Table V [25]	Table VIII [25]	HQS [36]	χ-SU(3) [36]	Resonance
h_0	0.01	0.01	0.03	0.03	0
h_1	0.42	0.42	0.43	0.43	0.4
h_{24}	$-0.10^{+0.05}_{-0.06}$	$0.10^{+0.05}_{-0.06}$	-0.12 ± 0.05	-0.14 ± 0.04	0
h_{35}	$0.25^{+0.13}_{-0.13}$	$0.26^{+0.09}_{-0.10}$	0.23 ± 0.09	0.12 ± 0.08	$[-1.4, 0.1]$
h_4'	$-0.32^{+0.35}_{-0.34}$	$-0.30^{+0.31}_{-0.28}$	-0.20 ± 0.31	-0.83 ± 0.30	0
h_5'	$-1.88^{+0.63}_{-0.61}$	$-1.94^{+0.46}_{-0.38}$	-1.82 ± 0.57	-1.00 ± 0.40	$[-0.7, 0]$

the combinations of the LECs are given in Eq. (4).[5] The following observations can be made:

(i) Provided that a positive value of c_m is chosen, h_1 is saturated by the light scalar exchange, which is similar to the LEC c_1 in the πN case [15]. The value of h_1 is fixed through the mass difference between strange and nonstrange charmed mesons, which is then adopted in these fits. One sees that the estimate here is in a good agreement with the empirical value. The agreement in turn might indicate that the model estimate for g_{DDS} is reasonable.

(ii) Because we only have the absolute values for g_V and g_T, one sees that the estimates from exchanging resonances are roughly consistent with those determined from the various NLO UChPT fits, while there are tensions when comparing with those from the NNLO UChPT fits in Ref. [37]. While there are quite a few fit parameters at NNLO, not many lattice data exist. On the one hand, more lattice calculations on observables for the scattering processes between heavy mesons and light mesons would be welcome to better pin down the LECs at NNLO. On the other hand, as pointed out in Ref. [12], the values of the LECs, which are scale dependent in general, are dominated by the resonances only when the renormalization scale μ is not too far away from the resonance region. The NLO fit results are obtained with $\mu = 1$ GeV, i.e., the scale appearing in the subtraction constant $a(\mu)$, which is around the masses of the light vector and scalar resonances. However, the NNLO fit results in Ref. [37] are obtained by setting $\mu = \overline{M}_D = 1.92$ GeV for convenience. Note that the scale dependence of the NNLO LECs stems both from the renormalization of the one-loop amplitude using EOMS scheme and the unitarization procedure accompanied by the subtraction constant $a(\mu)$.

[5]The notations of the LECs adopted in Ref. [36] are connected to ours by $h_0 = 2c_0$, $h_1 = -2c_1$,

$$h_{24} = 2\left[c_{24} + 2c_4\left(1 - \frac{\bar{M}_D^2}{m_P^2}\right)\right],$$
$$h_{35} = -2\left[c_{35} + 2c_5\left(1 - \frac{\bar{M}_D^2}{m_P^2}\right)\right], \qquad h_4' = -4c_4\frac{\bar{M}_D^2}{m_P^2},$$
$$h_5' = 2c_5\frac{\bar{M}_D^2}{m_P^2},$$

with $m_P = 1.9721$ GeV specified in Ref. [36] and $\bar{M}_D = (M_D^{\rm phy} + M_{D_s}^{\rm phy})/2$.

III. POSITIVITY CONSTRAINTS ON THE $D\phi$ INTERACTIONS

In this section, positivity constraints on the $D\phi$ interactions will be derived by using basic axiomatic principles of S-matrix theory, such as unitarity, analyticity, and crossing symmetry. Such constraints are important in the sense that model-independent information for the $D\phi$ interactions is provided. When employed in ChPT, they are translated into a much more practical form, i.e., positivity bounds on the LECs. In general, these involved LECs are unknown and not fixed by chiral symmetry. Furthermore, the number of the LECs increases when going to higher orders. Therefore, such bounds are of great use, especially for those which cannot be measured directly in experiments such as the $D\phi$ interactions under consideration. In what follows, details on the derivation of these constraints as well as practical applications of the bounds on the $D\phi$ interactions will be presented.

A. Positivity constraints implied by dispersion relations

For elastic $D\phi$ scattering, the Mandelstam triangle is the region bounded by $s = (M_D + M_\phi)^2$, $u = (M_D + M_\phi)^2$ and $t = 4M_\phi^2$ in the Mandelstam plane as displayed in Fig. 1. Inside the Mandelstam triangle, the scattering amplitude is analytic and real; see, e.g., Ref. [61] for an early application in the context baryon ChPT. Following Refs. [41,45], we restrict ourselves to the upper part of the Mandelstam triangle with $t \geq 0$. Using unitarity, analyticity, and crossing symmetry, an n-time subtracted fixed-t dispersion relation for the elastic $D\phi$ scattering amplitude with definite (S, I) can be written as

TABLE III. Comparison of the values of the LECs from the estimate using resonances with those from various fits to lattice data in unitarized ChPT at NNLO.

LEC	UχPT-6a [37]	UχPT-6b [37]	UχPT-6a' [37]	UχPT-6b' [37]	Resonance
h_0	0.02	0.02	0.02	0.02	0
h_1	0.43	0.43	0.43	0.43	0.4
h_{24}	$0.79^{+0.10}_{-0.09}$	$0.76^{+0.10}_{-0.09}$	$0.83^{+0.11}_{-0.10}$	$0.80^{+0.10}_{-0.10}$	0
h_{35}	$0.73^{+0.50}_{-0.38}$	$0.81^{+0.95}_{-0.62}$	$0.43^{+0.23}_{-0.23}$	$0.40^{+0.33}_{-0.29}$	$[-1.4, 0.1]$
h'_4	$-1.49^{+0.55}_{-0.57}$	$-1.56^{+0.61}_{-0.65}$	$-1.33^{+0.60}_{-0.60}$	$-1.72^{+0.64}_{-0.63}$	0
h'_5	$-11.47^{+2.24}_{-2.79}$	$-15.38^{+4.81}_{-7.20}$	$-4.25^{+0.65}_{-0.66}$	$-2.60^{+0.84}_{-0.87}$	$[-0.7, 0]$
g'_1[GeV^{-1}]	$-1.66^{+0.31}_{-1.59}$	$-2.44^{+0.57}_{-0.64}$	$-1.10^{+0.18}_{-0.23}$	$-1.90^{+0.58}_{-0.35}$	$[-0.2, -0.1]$
g_{23} [GeV^{-1}]	$-1.24^{+0.28}_{-1.51}$	$-2.00^{+0.52}_{-0.51}$	$-0.70^{+0.19}_{-0.24}$	$-1.48^{+0.61}_{-0.37}$	$[-0.5, -0.2]$
g'_3 [GeV^{-1}]	$2.12^{+0.55}_{-0.45}$	$2.85^{+1.41}_{-0.96}$	$0.98^{+0.15}_{-0.14}$	$0.58^{+0.20}_{-0.19}$	0.14

$$\frac{\mathrm{d}^n}{\mathrm{d}s^n}\mathcal{M}^{(S,I)}_{D\phi\to D\phi}(s,t) = \frac{n!}{\pi}\int_{(M_D+M_\phi)^2}^{+\infty}\mathrm{d}x'\left[\delta^{II'}\frac{\mathrm{Im}\mathcal{M}^{(S,I')}_{D\phi\to D\phi}(x'+i\epsilon,t)}{(x'-s)^{n+1}} + (-1)^n C^{II'}_{us}\frac{\mathrm{Im}\mathcal{M}^{(S,I')}_{D\overline{\phi}\to D\overline{\phi}}(x'+i\epsilon,t)}{(x'-u)^{n+1}}\right], \tag{20}$$

where $\overline{\phi}$ denotes the antiparticle of ϕ, and $C^{II'}_{us}$ represents the $u-s$ crossing matrix which is defined as

$$\mathcal{A}^I(u,t,s) = C^{II'}_{us}\mathcal{A}^{I'}(s,t,u), \tag{21}$$

where we have written explicitly all of the three Mandelstam variables so as to make the $u-s$ crossing explicit, and C_{su} is defined by exchanging the s- and u-channel amplitudes in the above equation. The matrices satisfy $C^{II'}_{us}C^{I'J}_{su} = \delta^{IJ}$. We want to mention that the imaginary part of $\mathcal{M}$ is positive definite above threshold.[6] Besides, we have assumed that all the processes involved in the dispersion relation are single-channel interactions such that the integration starts at the corresponding thresholds. The case with multichannel interactions will be discussed later. Both imaginary parts in the brackets in Eq. (20) are positive definite when x' is above threshold, i.e., $x' > (M_D+M_\phi)^2$.[7] In addition, the s-channel coefficient $\delta^{II'}$ is always non-negative. However, the u-channel one $(-1)^n C^{II'}_{us}$ is sometimes not. The aim is therefore to construct certain combinations of the $D\phi$ amplitudes with different isospins such that

$$\frac{\mathrm{d}^n}{\mathrm{d}s^n}[\alpha^I\mathcal{M}^{(S,I)}_{D\phi\to D\phi}(s,t)] \geq 0, \tag{22}$$

where summation over I is assumed. In combination with Eq. (20), a sufficient condition for the above positivity condition to hold is given by

$$\alpha^I\delta^{II'} \geq 0, \qquad \alpha^I C^{II'}_{us} \geq 0 \quad \text{(for even } n\text{)}. \tag{23}$$

For the multichannel case, all the cuts from the coupled channels need to be taken into account, and the integration should start from the lowest threshold. Taking the process $DK\to DK$ as an example, the integration in the $(S,I)=(1,1)$ channel will start at the $D_s\pi$ threshold rather than its physical DK threshold. Since the imaginary part $\mathrm{Im}T^{(1,1)}_{DK\to DK}(x'+i\epsilon,t)$ could be negative in the region $x'\in[(M_{D_s}+M_\pi)^2,(M_D+M_K)^2]$, the positivity condition in Eq. (22) is not applicable any more. However, as discussed in Ref. [42], in the multichannel case, the positivity conditions hold for processes of the type $a+b\to a+b$ such that m_a+m_b is the lightest threshold for both the s and u channels. This statement is obtained from the condition that the dispersion relation in Eq. (20) is true and that $t\geq 0$, which ensures the positivity of the Legendre polynomials for all partial waves. For details, we refer to Sec. IV in Ref. [42]. With this statement, among all the $D\phi$ scattering channels, only $D\pi\to D\pi$ and $D_s\pi\to D_s\pi$ survive.

To derive positivity constraints on the $D\pi\to D\pi$ and $D_s\pi\to D_s\pi$ scattering amplitudes, we need to know the explicit forms of the $u-s$ crossing matrices for these two processes, which are

$$\mathcal{C}_{us} = \begin{pmatrix} -\frac{1}{3} & \frac{4}{3} \\ \frac{2}{3} & \frac{1}{3} \end{pmatrix}, \quad \text{for } D\pi\to D\pi, \quad \text{and}$$
$$\mathcal{C}_{us} = 1, \quad \text{for } D_s\pi\to D_s\pi. \tag{24}$$

For the $D\pi$ case, the matrix is arranged such that the first channel refers to $I=1/2$ and the second refers to $I=3/2$.

[6]Here, we follow the convention $S=\mathbf{1}+i(2\pi)^4\delta^{(4)}\times(\sum_i p_i-\sum_f p_f)\mathcal{M}$, to define the scattering amplitude $\mathcal{M}(s,t)$.

[7]Since for each partial wave ℓ, $\mathrm{Im}\mathcal{M}_\ell(s)=\frac{2|k|}{\sqrt{s}}|\mathcal{M}_\ell(s)|^2\geq 0$ above threshold and the Legendre polynomials $P_\ell(\cos\theta)\geq 0$ for $t\geq 0$ (or equivalently $\cos\theta\geq 1$), one has $\mathrm{Im}\mathcal{M}^{(S,I)}(s,t)=\sum_{\ell=0}^{\infty}(2\ell+1)P_\ell(t)\mathrm{Im}\mathcal{M}^{(S,I)}_\ell(s)\geq 0$.

From now on, we will focus on the $n = 2$ case, which is the minimal number of subtractions in the dispersion integral required by the Froissart bound [62].

For $D\pi \to D\pi$, the upper part of the Mandelstam triangle is $\mathcal{R}_{D\pi} = \{(s,t)|s \le (M_D + M_\pi)^2, s + t \ge (M_D - M_\pi)^2, 0 \le t \le 4M_\pi^2\}$. When $(s,t) \in \mathcal{R}_{D\pi}$, a sufficient condition for $\frac{d^2}{ds^2}\{\alpha^I \mathcal{M}^I_{D\pi\to D\pi}(s,t)\} \ge 0$ is given by $2\alpha^{3/2} \ge \alpha^{1/2} \ge 0$. We choose the following three combinations of $\alpha^{1/2}$ and $\alpha^{3/2}$ to get bounds on three physical scattering amplitudes,

$$\begin{cases} \alpha^{1/2} = 0, \alpha^{3/2} = 1: & -\frac{d^2}{ds^2}\mathcal{A}_{D^+\pi^+\to D^+\pi^+}(s,t) \ge 0, \\ \alpha^{1/2} = \frac{2}{3}, \alpha^{3/2} = \frac{1}{3}: & -\frac{d^2}{ds^2}\mathcal{A}_{D^0\pi^+\to D^0\pi^+}(s,t) \ge 0, \\ \alpha^{1/2} = \frac{1}{3}, \alpha^{3/2} = \frac{2}{3}: & -\frac{d^2}{ds^2}\mathcal{A}_{D^+\pi^0\to D^+\pi^0}(s,t) \ge 0, \end{cases} \quad (25)$$

with $\mathcal{A} = -\mathcal{M}$.

For $D_s\pi \to D_s\pi$, the upper part of the Mandelstam triangle is $\mathcal{R}_{D_s\pi} = \{(s,t)|s \le (M_{D_s} + M_\pi)^2, s + t \ge (M_{D_s} - M_\pi)^2, 0 \le t \le 4M_\pi^2\}$. When $(s,t) \in \mathcal{R}_{D_s\pi}$, a sufficient condition for $\frac{d^2}{ds^2}\{\alpha^I \mathcal{M}^I_{D_s\pi\to D_s\pi}(s,t)\} \ge 0$ is $\alpha^1 \ge 0$. Choosing $\alpha^1 = 1$, one has

$$-\frac{d^2}{ds^2}\mathcal{A}_{D_s^+\pi^+\to D_s^+\pi^+}(s,t) \ge 0. \quad (26)$$

In the above, we have written the constraints in terms of the scattering amplitudes which are either explicitly given in Ref. [37] or easily obtainable by using crossing symmetry and isospin symmetry. Hence, their analytical expressions up to NNLO are all known and can be inserted into the above inequalities to obtain bounds on the LECs, which will be discussed in the next section.

In the end, it is worth noting that the validity of Eqs. (25) and (26) strongly relies on the crossing symmetry. The unitarized amplitude used in Ref. [37] that respects the right-hand cut unitarity exactly, however, has the shortcoming of violating crossing symmetry. Thus, it is not suitable to be applied to test the positivity constraints in Eqs. (25) and (26) nor to derive positivity bounds on the LECs.

B. Positivity bounds on the LECs

The representation of the $D\phi$ scattering amplitudes in the manifestly Lorentz covariant framework obtained in Ref. [37] is suitable to obtain reliable bounds on the LECs, since it possesses the correct analytic behavior inside the Mandelstam triangle. In the covariant formalism for the $SU(3)$ case, the NLO (tree-level) $D\phi$ amplitudes were first given by Ref. [24] and then followed by Refs. [25,35,36]. In Ref. [37], a complete covariant calculation up to NNLO (the leading one-loop order) is presented using the EOMS subtraction scheme which guarantees proper analyticity and has the correct power counting. These amplitudes can be employed to derive positivity bounds on the LECs with the help of the inequalities given in Eqs. (25) and (26). Note that, throughout this work, we follow the notations of Ref. [25], and the results from other works with different notations can be easily adapted to ours.

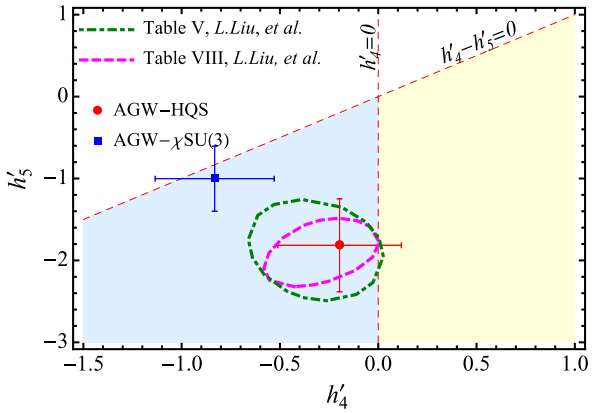

FIG. 3. Comparison of the NLO positivity bounds for h'_4 and h'_5 with their values obtained from fitting to the lattice data using unitarized ChPT at NLO. The positivity-bound region is depicted in light yellow bounded by the lines $h'_4 = 0$ and $h'_4 - h'_5 = 0$. The area in light blue denotes the region where the bound $h'_4 - h'_5 \ge 0$ is respected, while $h'_4 \ge 0$ is violated. The green dot-dashed and magenta dashed ellipses represent the 1-σ regions for h'_4 and h'_5 from the five- and four-parameter fits in Ref. [25], respectively. The red dot and blue square with error bars, denoted by AGW-HQS and AGW-χSU(3), respectively, are taken from Ref. [36].

1. Bounds up to $\mathcal{O}(p^2)$

Inserting the amplitudes up to NLO into Eqs. (25) and (26), the constraints on the scattering amplitudes turn into bounds on the LECs h_4 and h_5. Each inequality leads to one bound on the LECs. The intersection of all of the obtained bounds has a simple form:

$$\begin{cases} h_4 - h_5 \ge 0 \\ h_4 \ge 0 \end{cases}, \quad \text{or equivalently} \begin{cases} h'_4 - h'_5 \ge 0 \\ h'_4 \ge 0 \end{cases}. \quad (27)$$

Here, the parameters h_4 and h_5 are in units of GeV^{-2}, while h'_4 and h'_5, defined in Eq. (4), are dimensionless. The region restricted by the bounds on h'_4 and h'_5 in Eq. (27) is depicted as the light yellow area in Fig. 3. Two different sets of fitting values from Refs. [25,36] which resum the NLO scattering amplitudes in different ways are shown for comparison[8]:

(i) The first set is taken from Ref. [25]. There are two different fits: one with five parameters which are four LECs and one subtraction constant used to regularize the loop integral (cf. Table V therein) and the other with four parameters with the subtraction

[8]The results in Ref. [35] are not taken into consideration, since the preliminary lattice data [31], which are different from the final ones in Ref. [25], are used to perform fits there.

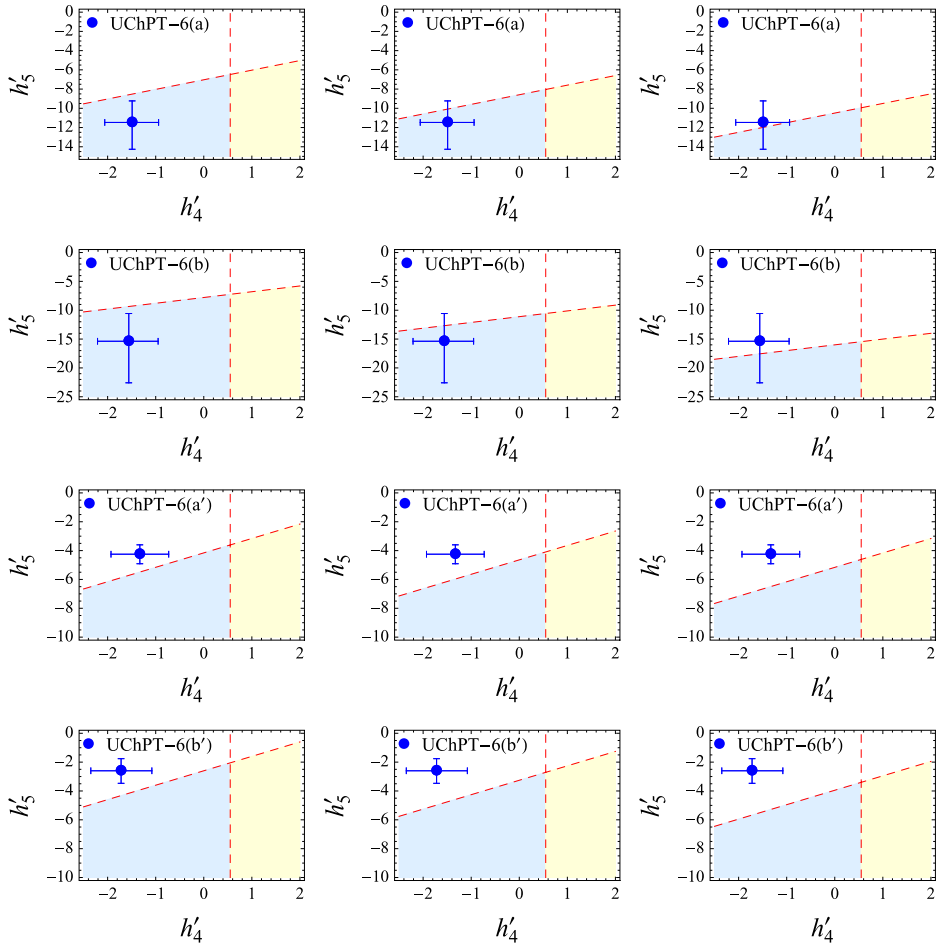

FIG. 4. Comparison of the positivity bounds for h_4' and h_5' with their six-channel NNLO fit values. The graphs in the first, second, and third column correspond to the case in which g_3' is fixed at its lowest, central, and largest values, respectively. The blue dots with error bars represent the fitting values of h_4' and h_5' from different fits: UChPT-6(a), UChPT-6(b), UChPT-6(a'), and UChPT-6(b'); see Ref. [37]. The NNLO positivity-bound region is in light yellow bounded by the lines $h_4' = 0.55$ and $h_4' - h_5' = g(g_3')$. The area in light blue denotes the region where the bound $h_4' - h_5' \geq g(g_3')$ is respected, while $h_4' \geq 0.55$ is violated.

constant fixed from reproducing the $D_{s0}^*(2317)$ mass in the $(S, I) = (1, 0)$ channel (cf. Table VIII therein). The 1-σ regions, with the parameter correlations in the fits taken into account, from these two fits for the values for h_4' and h_5' are shown by the regions surrounded by the green dot-dashed line (for the five-parameters fit) and by the magenta dashed line (for the four-parameter fit).

(ii) The second set is taken from Ref. [36]. In that work, a special renormalization scheme is proposed to deal with the so-called power-counting breaking terms appearing in the loop functions. In Fig. 3, the blue square and red dot represent the fit values taken from χ-SU(3) fit and HQS fit, which correspond to different regularizations of the scalar two-point loop integral, in Ref. [36], respectively.

As can be seen from Fig. 3, the fit values from Ref. [25] are only marginally consistent with the region allowed by the bounds. The LEC values from the HQS fit in Ref. [36] have a small overlap with the positivity bound, while the ones from the χ-SU(3) fit are completely outside the region derived from positivity.

2. Bounds up to $\mathcal{O}(p^3)$

Inserting the $D\phi$ amplitudes up to NNLO into the positivity constraints in Eqs. (25) and (26), one gets bounds on the LECs at the NNLO level, which are

$$\begin{cases} h_4 - h_5 - 24 M_D \nu_D g_3 \geq f^{(2)}_{D^+\pi^+ \to D^+\pi^+}(s,t), & (s,t) \in \mathcal{R}_{D\pi}, \\ h_4 - h_5 + 24 M_D \nu_D g_3 \geq f^{(2)}_{D^0\pi^+ \to D^0\pi^+}(s,t), & (s,t) \in \mathcal{R}_{D\pi}, \\ h_4 - h_5 \geq f^{(2)}_{D^+\pi^0 \to D^+\pi^0}(s,t), & (s,t) \in \mathcal{R}_{D\pi}, \\ h_4 \geq f^{(2)}_{D_s^+\pi^+ \to D_s^+\pi^+}(s,t), & (s,t) \in \mathcal{R}_{D_s\pi}, \end{cases} \tag{28}$$

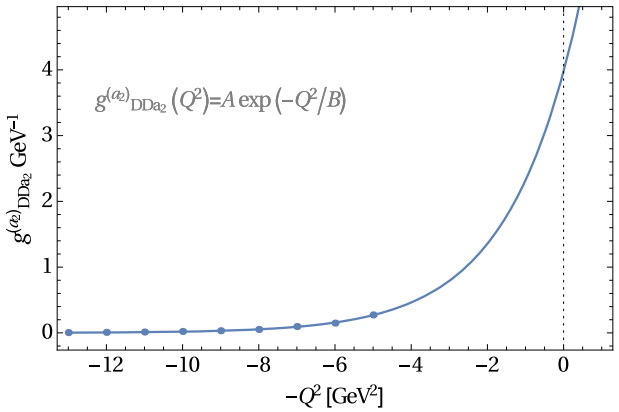

FIG. 5. Momentum dependence of the DDa_2 form factor (for off-shell a_2). The dots give the results from QCD sum rules, and the solid line gives the extrapolation.

where

$$\nu_D \equiv \frac{s-u}{4M_D}, \quad \text{and} \quad f^{(2)}_{\text{process}}(s,t) \equiv \frac{F_\pi^2}{2}\frac{\mathrm{d}^2}{\mathrm{d}s^2}\mathcal{A}^{\text{loop}}_{\text{process}}(s,t).$$

Each bound would become more stringent if one always sets $f^{(2)}_{\text{process}}(s,t)$ at its maximum inside $\mathcal{R}_{D\pi}$ (or $\mathcal{R}_{D_s\pi}$). Numerically, we find

$$\begin{aligned}&\max\{f^{(2)}_{D^+\pi^+\to D^+\pi^+}(s,t)\} = \max\{f^{(2)}_{D^0\pi^+\to D^0\pi^+}(s,t)\} = 0.34,\\ &\max\{f^{(2)}_{D^+\pi^0\to D^+\pi^0}(s,t)\} = 0.28\end{aligned} \tag{29}$$

in the region $(s,t) \in \mathcal{R}_{D\pi}$ and

$$\max\{f^{(2)}_{D_s^+\pi^+\to D_s^+\pi^+}(s,t)\} = 0.15 \tag{30}$$

in the region $(s,t) \in \mathcal{R}_{D_s\pi}$. By further using the condition $|\nu_D| \le \nu_D^{\text{th}}(t) = M_\pi + t/4M_D \le M_\pi + M_\pi^2/M_D$, one finally obtains the bounds

$$\begin{cases} h_4' - h_5' - 24|g_3'|(M_D+M_\pi)M_\pi/\overline{M}_D \ge 1.25, \\ h_4' \ge 0.55, \end{cases} \tag{31}$$

which are expressed in terms of h_4', h_5', and g_3'. Comparing with the $\mathcal{O}(p^2)$ bounds given in Eq. (27), the $\mathcal{O}(p^3)$ bounds are much more stringent.

To compare the values of h_4' and h_5' from the fits to the lattice data using unitarized ChPT at NNLO with these bounds, we choose to fix g_3' at three typical values: the central and the two extremes within the 1-σ region of each fit. For convenience, we define a function of g_3', $g(g_3') \equiv 1.25 + 24|g_3'|(M_D+M_\pi)M_\pi/\overline{M}_D$ and rewrite the bounds in Eq. (31) as

$$\begin{cases} h_4' - h_5' \ge g(g_3'), \\ h_4' \ge 0.55. \end{cases} \tag{32}$$

Notice that the bounds depend on the renormalization scale μ since the loop contributions $f^{(2)}_{\text{process}}(s,t)$ are involved. The NNLO bounds in Eqs. (31) and (32) are obtained by setting $\mu = \overline{M}_D$ in accordance with Ref. [37]. The comparison is shown in Fig. 4. The bounds displayed in the graphs in the first, second, and third columns correspond to taking the central, the lowest, and the largest values in each fit for g_3', respectively. As seen from the plots, no fit completely obeys the bounds. For UChPT-6(a) and UChPT-6(b), the fit values are consistent with the first bound in Eq. (31), while they violate the second one, i.e., the one restricting h_4' only. Both bounds are violated in the fits for UChPT-6(a') and UChPT-6(b'), which are the ones with a prior, which requires all of the LECs (made dimensionless) to take natural values of order $\mathcal{O}(1)$.

These comparisons, however, have to be interpreted with caution. The positivity bounds in Eqs. (27) and (31) were derived using the perturbative scattering amplitudes, while the fits in Refs. [25,36,37] were performed using resummed amplitudes with perturbative kernels. The resummed amplitudes using various unitarization approaches in the literature break the crossing symmetry, which, however, is one of the main components in deriving the positivity bounds through dispersion relations. It is thus not surprising that the LECs determined in the UChPT fits do not respect the positivity bounds. Nevertheless, we notice that all of these fits prefer a negative value for h_4, while the positivity bound requires it to be positive.

IV. SUMMARY AND OUTLOOK

We have estimated the LECs in the NLO and NNLO chiral Lagrangian for the $D\phi$ interaction using resonance exchanges. These LECs receive contributions from exchanging the scalar charmed mesons, the light-flavor vector, scalar, and tensor mesons. We found that h_1 is entirely saturated by the light scalar-meson exchange. The resulting estimates are consistent with the NLO UChPT fitting results [25,36], while sizeable deviations from the determinations with the NNLO UChPT [37] are found. More lattice data on the $D\phi$ scattering observables would be useful to better pin down the LECs at NNLO.

In parallel, with the help of axiomatic S-matrix principles, such as unitarity, analyticity, and crossing symmetry, we derived positivity constraints on the $D\pi$ and $D_s\pi$ scattering amplitudes in upper parts of Mandelstam triangles, $\mathcal{R}_{D\pi}$ and $\mathcal{R}_{D_s\pi}$, respectively. In combination with the corresponding scattering amplitudes calculated in ChPT using the EOMS scheme, the constraints are then translated into a set of bounds on the LECs. At order $\mathcal{O}(p^2)$, the

bounds are independent of the Mandelstam variables s, t and hence have unique forms throughout $\mathcal{R}_{D\pi}$ or $\mathcal{R}_{D_s\pi}$. At order $\mathcal{O}(p^3)$, the most stringent bounds are obtained by zooming inside the upper part of the Mandelstam triangle such that they can easily be employed and implemented to constrain future analyses. Finally, as a first use of these bounds, the values of LECs in the literature are compared with them. The comparison shows that the bounds, in particular the one constraining h_4 only, are badly violated in all the previous determinations from fitting to lattice data using UChPT. The most probable reason for this is that the UChPT amplitudes violate crossing symmetry which is the basis of deriving the positivity bounds.

For a more reasonable comparison, one needs to derive positivity bounds for the unitarized amplitudes. One possible attack to the problem could come from using the method proposed in Ref. [63] where the author proposed a crossing-symmetric amplitude for the process $\gamma\pi \to \pi\pi$ combining the inverse amplitude method, which is one of the unitarization approaches, and the Roy equation. In our case, the problem is much more involved due to different masses and coupled channels. Whether such a method can lead to a feasible procedure still needs to be seen.

ACKNOWLEDGMENTS

We would like to thank Z.-H. Guo and W. Chen for helpful discussions. This work is supported in part by DFG and NSFC through funds provided to the Sino-German CRC 110 "Symmetries and the Emergence of Structure in QCD" (DFG TRR 110, NSFC Grant No. 11621131001), by the Thousand Talents Plan for Young Professionals, by the CAS Key Research Program of Frontier Sciences (Grant No. QYZDB-SSW-SYS013), and by the CAS President's International Fellowship Initiative (Grant No. 2015VMA076).

APPENDIX A: LO BORN AMPLITUDES

In this Appendix, the LO Born amplitudes for various resonance exchanges are listed for completeness. For a given amplitude, we use capital subscripts, S, T, and U, to label the channels and superscripts, D_0^*, V (vector) and S (scalar), to mark which resonance is exchanged. The coefficients appearing in the amplitudes are listed in Table IV:

(i) D_0^* exchange ($m = \mathring{M}_{D_0^*}$):

$$\mathcal{A}_S^{D_0^*}(s,t,u) = \mathcal{C}_S^{D_0^*}\frac{g_0^2}{F_0^2}\frac{p_1\cdot p_2 p_3\cdot p_4}{s-m^2},$$
$$\mathcal{A}_U^{D_0^*}(s,t,u) = \mathcal{C}_U^{D_0^*}\frac{g_0^2}{F_0^2}\frac{p_1\cdot p_4 p_2\cdot p_3}{u-m^2}. \quad \text{(A1)}$$

(ii) Light-flavor vector meson exchange:

$$\mathcal{A}_T^V(s,t,u) = C_T^V\frac{g_{DDV}g_V}{F_0^2} \times\left\{\frac{(p_1-p_3)\cdot p_2(p_1+p_3)\cdot p_4}{M_V^2-t} - (p_2\leftrightarrow p_4)\right\}. \quad \text{(A2)}$$

(iii) Light-flavor scalar meson exchange:

$$\mathcal{A}_T^S(s,t,u) = \frac{2g_{DDS}\{\mathcal{C}_{T,m}^{S8} - \mathcal{C}_{T,d}^{S8}p_2\cdot p_4\}}{3F_0^2(M_{S8}^2-t)} + \frac{4\tilde{g}_{DDS}\{\mathcal{C}_{T,m}^{S1} - \mathcal{C}_{T,d}^{S1}p_2\cdot p_4\}}{F_0^2(M_{S1}^2-t)}. \quad \text{(A3)}$$

APPENDIX B: ESTIMATE OF THE TENSOR RESONANCE CONTRIBUTION TO THE LEC h_5

In this Appendix, we use the technique in Refs. [12,13], which is different from but equivalent to the one used in the main text, to estimate the contribution of exchanging the light tensor mesons, denoted by T, with $J^{PC} = 2^{++}$ to the LEC h_5. We construct the Lagrangian for the DDT coupling as

$$\mathcal{L}_{DDT} = g_{DDT}\mathcal{D}_\mu D T^{\mu\nu}\mathcal{D}_\nu D^\dagger. \quad \text{(B1)}$$

One could calculate the tensor-meson contribution to the LECs by integrating out the tensor meson field as follows.

The $J^{PC} = 2^{++}$ mesons are described by the symmetric Hermitian field [59],

$$T_{\mu\nu} = T^0_{\mu\nu}\frac{\lambda_0}{\sqrt{2}} + \frac{1}{\sqrt{2}}\sum_{i=1}^{8}\lambda_i T^i_{\mu\nu}, \qquad T_{\mu\nu} = T_{\nu\mu}, \quad \text{(B2)}$$

where the singlet and octet components are

$$T^0 = f_2^0, \quad \text{and}$$
$$\frac{1}{\sqrt{2}}\sum_{i=1}^{8}\lambda_i T^i = \begin{pmatrix} \frac{a_2^0}{\sqrt{2}} + \frac{f_2^8}{\sqrt{6}} & a_2^+ & K_2^{*+} \\ a_2^- & -\frac{a_2^0}{\sqrt{2}} + \frac{f_2^8}{\sqrt{6}} & K_2^{*0} \\ K_2^{*-} & \overline{K}_2^{*0} & -\frac{2f_2^8}{\sqrt{6}} \end{pmatrix}, \quad \text{(B3)}$$

respectively.

The coupling of a single tensor meson to the Goldstone bosons can be described by the Lagrangian [59]

$$\mathcal{L} = -\frac{1}{2}\langle T_{\mu\nu}D_T^{\mu\nu,\rho\sigma}T_{\rho\sigma}\rangle + \langle T_{\mu\nu}J_T^{\mu\nu}\rangle,$$
$$J_T^{\mu\nu} \equiv g_T\{u^\mu, u^\nu\}, \quad \text{(B4)}$$

TABLE IV. Coefficients for the resonance-exchange amplitudes.

Physical processes	$\mathcal{C}_S^{D_0^*}$	$\mathcal{C}_U^{D_0^*}$	$\mathcal{C}_T^V$	$\mathcal{C}_{T,m}^{S8}$	$\mathcal{C}_{T,d}^{S8}$	$\mathcal{C}_{T,m}^{S1}$	$\mathcal{C}_{T,d}^{S1}$
$D^0K^- \to D^0K^-$	0	2	$\sqrt{2}$	M_K^2	1	M_K^2	1
$D^+K^+ \to D^+K^+$	0	0	0	$-2M_K^2$	-2	M_K^2	1
$D^+\pi^+ \to D^+\pi^+$	0	2	$\sqrt{2}$	M_π^2	1	M_π^2	1
$D^+\eta \to D^+\eta$	$\frac{1}{3}$	$\frac{1}{3}$	0	$\frac{1}{3}(5M_\pi^2 - 8M_K^2)$	-1	M_η^2	1
$D_s^+K^+ \to D_s^+K^+$	0	2	$\sqrt{2}$	M_K^2	1	M_K^2	1
$D_s^+\eta \to D_s^+\eta$	$\frac{4}{3}$	$\frac{4}{3}$	0	$\frac{2}{3}(8M_K^2 - 5M_\pi^2)$	2	M_η^2	1
$D_s^+\pi \to D_s^+\pi$	0	0	0	$-2M_\pi^2$	-2	M_π^2	1
$D^0\eta \to D^0\pi^0$	$\sqrt{\frac{1}{3}}$	$\sqrt{\frac{1}{3}}$	0	$\sqrt{3}M_\pi^2$	$\sqrt{3}$	0	0
$D_s^+K^- \to D^0\pi^0$	$\sqrt{2}$	0	-1	$\frac{3}{2\sqrt{2}}(M_K^2 + M_\pi^2)$	$\frac{3}{\sqrt{2}}$	0	0
$D_s^+K^- \to D^0\eta$	$\sqrt{\frac{2}{3}}$	$-2\sqrt{\frac{2}{3}}$	$-\sqrt{3}$	$\sqrt{\frac{3}{8}}(3M_\pi^2 - 5M_K^2)$	$-\sqrt{\frac{3}{2}}$	0	0

where $J_T^{\mu\nu}$ is the tensor current and

$$D_T^{\mu\nu,\rho\sigma} = (\mathcal{D}^2 + M_T^2)\left[\frac{1}{2}(g^{\mu\rho}g^{\nu\sigma} + g^{\mu\sigma}g^{\nu\rho}) - g^{\mu\nu}g^{\rho\sigma}\right] + g^{\rho\sigma}\mathcal{D}^\mu\mathcal{D}^\nu + g^{\mu\nu}\mathcal{D}^\rho\mathcal{D}^\sigma - \frac{1}{2}(g^{\nu\sigma}\mathcal{D}^\mu\mathcal{D}^\rho + g^{\rho\nu}\mathcal{D}^\mu\mathcal{D}^\sigma + g^{\mu\sigma}\mathcal{D}^\rho\mathcal{D}^\nu + g^{\rho\mu}\mathcal{D}^\sigma\mathcal{D}^\nu). \tag{B5}$$

Inserting the equation of motion for the tensor mesons, $T_{\rho\sigma} = (D^{\mu\nu,\rho\sigma})^{-1}J_T^{\mu\nu}$, into $\mathcal{L}_{DDT}$, we get

$$\mathcal{L}_{DDT} = \mathcal{L}_{DDT}^{(2)} + O(p^4),$$
$$\mathcal{L}_{DDT}^{(2)} = \frac{g_{DDT}}{M_T^2}\mathcal{D}_\mu D J_T^{\mu\nu}\mathcal{D}_\nu D^\dagger = \frac{g_{DDT}g_T}{M_T^2}\mathcal{D}_\mu D\{u^\mu, u^\nu\}\mathcal{D}_\nu D^\dagger. \tag{B6}$$

It is then easy to see that the light-tensor mesons only contribute to the LEC h_5, and the contribution is

$$h_5^T = \frac{g_{DDT}g_T}{M_T^2}. \tag{B7}$$

APPENDIX C: ESTIMATE OF THE COUPLING CONSTANT g_{DDT} VIA QCD SUM RULES

In this Appendix, we estimate the unknown off-shell coupling constant g_{DDT} using QCD sum rules, following the procedure in, e.g., Refs. [64,65]. To be specific, we will calculate the $D^0D^-a_2^+$ coupling. The standard procedure for computing a coupling constant in the method of QCD sum rules is to consider the three-point correlation function, which in our case is given by

$$\Pi_{\mu\nu}(p', p, q) = i^2\int d^4x\int d^4y e^{i(-p'x+yp)} \times \langle 0|T\{j^{D^0}(x)j^{D^-}(y)j_{\mu\nu}^{a_2^+}(0)\}|0\rangle, \tag{C1}$$

where $q = p' - p$ denotes the momentum transfer. The interpolating currents that we use for the D^0, D^-, and a_2^+ mesons are

$$j^{D^0}(x) = i\bar{u}(x)\gamma_5 c(x),$$
$$j^{D^-}(x) = i\bar{c}(x)\gamma_5 d(x),$$
$$j_{\mu\nu}^{a_2^+}(x) = \frac{i}{2}\bar{d}(x)(\gamma_\mu\overleftrightarrow{D}_\nu + \gamma_\nu\overleftrightarrow{D}_\mu)u(x), \tag{C2}$$

where $\overleftrightarrow{D}_\mu = (\vec{D}_\mu - \overleftarrow{D}_\mu)/2$.

One can calculate the correlation function in two different ways. On the one hand, the correlation function in Eq. (C1) can be computed by inserting a complete set of appropriate hadronic states with the same quantum numbers as the interpolating currents. Following the usual procedure, we obtain

$$\Pi_{\mu\nu}^{\rm had}(p'^2, p^2, q^2) = \frac{\langle 0|j^{D^0}|D^0(p')\rangle\langle 0|j^{D^-}|D^-(p)\rangle\langle 0|j_{\mu\nu}^{a_2^+}|a_2^+(q,\epsilon)\rangle}{(p'^2 - m_D^2)(p^2 - m_D^2)(q^2 - m_a^2)} \times \langle D^0(p')a_2^+(q,\epsilon)|D^+(p)\rangle + \cdots, \tag{C3}$$

where the ellipses represent the contributions of the excited states and the continuum. The matrix elements above are parametrized as [65]

$$\langle 0|j^D|D(p)\rangle = i\frac{m_D^2 f_D}{m_c + m_q},$$
$$\langle 0|j_{\mu\nu}^{a_2^+}|a_2^+(q,\epsilon)\rangle = m_a^3 f_a \epsilon_{\mu\nu}^{*(\lambda)},$$
$$\langle D^0(p')a_2^+(q,\epsilon)|D^+(p)\rangle = g_{DDa_2}\epsilon_{\alpha\beta}^{(\lambda)}p'_\alpha p_\beta, \tag{C4}$$

where f_D and f_a are the decay constants of $D^0(D^-)$ and a_2^+ mesons and g_{DDa_2} is the form factor of the DDT coupling under consideration. Substituting the above matrix elements into Eq. (C3), the correlation function takes the form

$$\Pi^{\rm had}_{\mu\nu}(p'^2,p^2,q^2)=i^2\left(\frac{m_D^2 f_D}{m_c+m_q}\right)^2\frac{g_{DDa_2}f_a m_a^3}{(p'^2-m_D^2)(p^2-m_D^2)(q^2-m_a^2)}\times\left\{1-\frac{1}{3m_a^2}(p^2+p'^2+2q^2)-\frac{1}{3m_a^4}[(p^2-p'^2)^2-(q^2)^2]\right\}(p'^\mu p^\nu+p'^\nu p^\mu)+\cdots, \tag{C5}$$

where only the Lorentz structure $(p'^\mu p^\nu+p'^\nu p^\mu)$ is kept, and the following relation has been used,

$$\sum_\lambda \epsilon^{(\lambda)}_{\mu\nu}\epsilon^{*(\lambda)}_{\alpha\beta}=\frac{1}{2}T_{\mu\alpha}T_{\nu\beta}+\frac{1}{2}T_{\mu\beta}T_{\nu\alpha}-\frac{1}{3}T_{\mu\nu}T_{\alpha\beta}, \tag{C6}$$

with $T_{\mu\nu}=-g_{\mu\nu}+q_\mu q_\nu/m_a^2$.

On the other hand, the correlation function can be calculated at the quark-gluon level using the QCD operator product expansion (OPE) method. It is convenient to evaluate it in the fixed-point gauge, $(x-x_0)^\mu A^a_\mu(x)=0$, where x_0 is an arbitrary point in the coordinate space and could be chosen at the origin. Then, in the deep Euclidean region, the potential can be expressed in terms of the field strength tensor $G_{\mu\nu}=\lambda^a G^a_{\mu\nu}/2$ as [66]

$$A_\mu(x)=\frac{1}{2}x^\nu G_{\nu\mu}(0)+\frac{1}{3}x^\alpha x^\nu D_\alpha G_{\nu\mu}(0)+\mathcal{O}(x^3). \tag{C7}$$

Since we are not aiming at a precise calculation, we will only keep the vacuum condensate of the lowest dimension, that is the quark condensate. Considering only the Lorentz structure $(p'^\mu p^\nu+p'^\nu p^\mu)$ and using the double dispersion relation, we find

$$\Pi_{\mu\nu}(p'^2,p^2,q^2)=\Pi(p'^2,p^2,q^2)(p'^\mu p^\nu+p'^\nu p^\mu)+\cdots, \tag{C8}$$

$$\Pi(p'^2,p^2,q^2)=\int ds_1 ds_2\frac{\rho^{\rm pert}(s_1,s_2,q^2)}{(s_1-p'^2)(s_2-p^2)}+\Pi^{qq}(p'^2,p^2,q^2), \tag{C9}$$

where

$$\rho^{\rm pert}(s_1,s_2,q^2)=-\frac{3}{8\pi^2\lambda^{5/2}}(s_1+s_2-t-2m_c^2)\{(s_1s_2+m_c^4)(\lambda+3t(s_1+s_2-t))-3m_c^2(s_1+s_2-t)[(s_1-s_2)^2-t(s_1+s_2)]\}, \tag{C10}$$

with $\lambda=(s_1+s_2-t)^2-4s_1s_2$, and

$$\Pi^{qq}(p'^2,p^2,q^2)=\frac{1}{4}m_c\langle\bar{q}q\rangle\left(\frac{1}{p'^2-m_c^2}+\frac{1}{p^2-m_c^2}\right)\frac{1}{q^2}. \tag{C11}$$

To suppress the contribution from the excited states, we perform a double Borel transformation in both variables p'^2 and p^2 to the correlation functions in Eqs. (C5) and (C9). Using the quark-hadron duality, we obtain

$$\Pi(M_B^2,M_B'^2,q^2)=i^2\frac{g_{DDa_2}f_a m_a^3}{q^2-m_a^2}\left(\frac{m_D^2 f_D}{m_c+m_q}\right)^2\left[1-\frac{2(q^2+m_D^2)}{3m_a^2}+\frac{q^4}{3m_a^4}\right]e^{-m_D^2/M_B^2-m_D^2/M_B'^2}=\int_{s_{1\,\rm min}}^{s_1^0}\int_{s_{2\,\rm min}}^{s_2^0}ds_1ds_2\rho^{\rm pert}(s_1,s_2,q^2)e^{-s_1/M_B^2-s_2/M_B'^2}. \tag{C12}$$

It is clear that the coupling g_{DDa_2} is in fact given by a form factor as a function of the Euclidean momentum $Q^2=-q^2$, which will be denoted by $g^{(a_2)}_{DDa_2}(Q^2)$, where the superscript means that the meson a_2^+ is off shell while the D mesons are on shell since the correlation function is evaluated in the spacelike region $Q^2>0$.

We neglect the light-quark masses and use the following values for numerical analysis: $m_c=1.27$ GeV, $m_D=1.87$ GeV, $m_a=1.32$ GeV, $\langle\bar{q}q\rangle=(-0.24)^3$ GeV, $f_D=0.207$ GeV [65], and $f_a=0.041$ [67]. Furthermore, $s_{1\,\rm min}=m_c^2$, and $s_{2\,\rm min}=\frac{m_c^2}{m_c^2-s_1}q^2+m_c^2$. Since the dependence of the form factor on M_B^2 and $M_B'^2$ is weak, one can set $M_B'^2=M_B^2$ [64].

The window for the Borel mass M_B^2 can be determined by requiring both the dominance of the ground-state hadronic poles and the convergence of the OPE. The quark condensate contribution would disappear if the double Borel transformation is performed in the variables p'^2 and p^2. To estimate the lower bound of M_B^2, we choose to perform the double Borel transformation in variables p^2 and q^2 and assume the lower bound is the same as that in the double Borel transformation in p'^2 and p^2. The lower limit of M_B^2 is estimated by requiring $|\Pi^{qq}(p'^2, M_B^2, M_B^2)/\Pi^{\rm pert}(p'^2, M_B^2, M_B^2)|$ to be smaller than 25% for Euclidean momentum p'^2. At the same time, the upper bound of the Borel mass M_B^2 can be estimated by requiring the pole contribution (PC) to be larger than 75%, which is defined by

$$\mathrm{PC} = \frac{\int_{s_{1\,\min}}^{s_1^0} ds_1 \int_{s_{2\,\min}}^{s_2^0} ds_2 \rho^{\rm pert}(s_1, s_2, q^2) e^{-s_1/M_B^2 - s_2/M_B^2}}{\int_{s_{1\,\min}}^{\infty} ds_1 \int_{s_{2\,\min}}^{\infty} ds_2 \rho^{\rm pert}(s_1, s_2, q^2) e^{-s_1/M_B^2 - s_2/M_B^2}}. \tag{C13}$$

The parameters s_1^0 and s_2^0 are chosen around the region where the variation of coupling constant $g_{DDa_2}^{(a_2)}(Q^2)$ is minimal. Given a value of Q^2, we obtain a corresponding $g_{DDa_2}^{(a_2)}(Q^2)$. From the above requirements, the Borel window we use here is $M_B^2 \sim [3.2\ \mathrm{GeV}^2, 4.0\ \mathrm{GeV}^2]$. We take $M_B^2 = 3.6\ \mathrm{GeV}^2$ for estimating the form factor $g_{DDa_2}^{(a_2)}(Q^2)$, and the values of s_1^0 and s_2^0 are chosen to increase slightly from around 6.0 to 8.5 GeV^2 as increasing Q^2 from 5 to 12 GeV^2. Since we are only able to calculate the form factor in the deep Euclidean region, we need to extrapolate it to $Q^2 = 0$ to get the coupling constant. The extrapolation is rather model dependent. To be specific, we simply take the form $g_{DDa_2}^{(a_2)}(Q^2) = A\exp(-Q^2/B)$ used in Refs. [64,68] despite that no physical reasoning is behind this parametrization. With this form, we fit to a few points in the Euclidean region and get $A = 10.1\ \mathrm{GeV}^{-1}$ and $B = 1.9\ \mathrm{GeV}^2$. The momentum dependence of the DDa_2 form factor is shown in Fig. 5. Finally, we get an estimate for the coupling constant as

$$g_{DDT} \approx g_{DDa_2}(0) \approx 3.9\ \mathrm{GeV}^{-1}. \tag{C14}$$

It should be noted that such an estimate bears a large uncertainty which we do not know how to quantify, and the resulting value can only be regarded as an order-of-magnitude estimate.

[1] S. Weinberg, Physica (Amsterdam) **96A**, 327 (1979).
[2] J. Gasser and H. Leutwyler, Ann. Phys. (N.Y.) **158**, 142 (1984).
[3] J. Gasser and H. Leutwyler, Nucl. Phys. **B250**, 465 (1985).
[4] N. Fettes, U.-G. Meißner, and S. Steininger, Nucl. Phys. **A640**, 199 (1998).
[5] N. Fettes and U.-G. Meißner, Nucl. Phys. **A676**, 311 (2000).
[6] Y.-H. Chen, D.-L. Yao, and H. Q. Zheng, Phys. Rev. D **87**, 054019 (2013).
[7] J. M. Alarcon, J. Martin Camalich, and J. A. Oller, Ann. Phys. (Amsterdam) **336**, 413 (2013).
[8] M. Hoferichter, J. Ruiz de Elvira, B. Kubis, and U.-G. Meißner, Phys. Rev. Lett. **115**, 192301 (2015).
[9] D. L. Yao, D. Siemens, V. Bernard, E. Epelbaum, A. M. Gasparyan, J. Gegelia, H. Krebs, and U.-G. Meißner, J. High Energy Phys. 05 (2016) 038.
[10] N. Fettes, V. Bernard, and U.-G. Meißner, Nucl. Phys. **A669**, 269 (2000).
[11] E. Epelbaum, H.-W. Hammer, and U.-G. Meißner, Rev. Mod. Phys. **81**, 1773 (2009).
[12] G. Ecker, J. Gasser, A. Pich, and E. de Rafael, Nucl. Phys. **B321**, 311 (1989).
[13] G. Ecker, J. Gasser, H. Leutwyler, A. Pich, and E. de Rafael, Phys. Lett. B **223**, 425 (1989).
[14] J. F. Donoghue, C. Ramirez, and G. Valencia, Phys. Rev. D **39**, 1947 (1989).
[15] V. Bernard, N. Kaiser, and U.-G. Meißner, Nucl. Phys. **A615**, 483 (1997).
[16] B. Aubert *et al.* (*BABAR* Collaboration), Phys. Rev. Lett. **90**, 242001 (2003).
[17] P. Krokovny *et al.* (Belle Collaboration), Phys. Rev. Lett. **91**, 262002 (2003).
[18] T. Barnes, F. E. Close, and H. J. Lipkin, Phys. Rev. D **68**, 054006 (2003).
[19] E. E. Kolomeitsev and M. F. M. Lutz, Phys. Lett. B **582**, 39 (2004).
[20] J. Hofmann and M. F. M. Lutz, Nucl. Phys. **A733**, 142 (2004).
[21] F.-K. Guo, P.-N. Shen, H.-C. Chiang, R.-G. Ping, and B.-S. Zou, Phys. Lett. B **641**, 278 (2006).
[22] D. Gamermann, E. Oset, D. Strottman, and M. J. Vicente Vacas, Phys. Rev. D **76**, 074016 (2007).
[23] F.-K. Guo, C. Hanhart, S. Krewald, and U.-G. Meißner, Phys. Lett. B **666**, 251 (2008).
[24] F.-K. Guo, C. Hanhart, and U.-G. Meißner, Eur. Phys. J. A **40**, 171 (2009).
[25] L. Liu, K. Orginos, F.-K. Guo, C. Hanhart, and U.-G. Meißner, Phys. Rev. D **87**, 014508 (2013).
[26] D. Mohler, C. B. Lang, L. Leskovec, S. Prelovsek, and R. M. Woloshyn, Phys. Rev. Lett. **111**, 222001 (2013).
[27] G. Moir, M. Peardon, S. M. Ryan, C. E. Thomas, and D. J. Wilson, J. High Energy Phys. 10 (2016) 011.

[28] G. Burdman and J. F. Donoghue, Phys. Lett. B **280**, 287 (1992).
[29] M. B. Wise, Phys. Rev. D **45**, R2188 (1992).
[30] T. M. Yan, H. Y. Cheng, C. Y. Cheung, G. L. Lin, Y. C. Lin, and H. L. Yu, Phys. Rev. D **46**, 1148 (1992); **55**, 5851 (1997).
[31] L. Liu, H.-W. Lin, and K. Orginos, *Proc. Sci.*, LATTICE2008 (2008) 112.
[32] D. Mohler, S. Prelovsek, and R. M. Woloshyn, Phys. Rev. D **87**, 034501 (2013).
[33] Y. R. Liu, X. Liu, and S. L. Zhu, Phys. Rev. D **79**, 094026 (2009).
[34] L. S. Geng, N. Kaiser, J. Martin-Camalich, and W. Weise, Phys. Rev. D **82**, 054022 (2010).
[35] P. Wang and X. G. Wang, Phys. Rev. D **86**, 014030 (2012).
[36] M. Altenbuchinger, L.-S. Geng, and W. Weise, Phys. Rev. D **89**, 014026 (2014).
[37] D.-L. Yao, M.-L. Du, F.-K. Guo, and U.-G. Meißner, J. High Energy Phys. 11 (2015) 058.
[38] Z.-H. Guo, U.-G. Meißner, and D.-L. Yao, Phys. Rev. D **92**, 094008 (2015).
[39] B. Ananthanarayan, D. Toublan, and G. Wanders, Phys. Rev. D **51**, 1093 (1995).
[40] P. Dita, Phys. Rev. D **59**, 094007 (1999).
[41] A. V. Manohar and V. Mateu, Phys. Rev. D **77**, 094019 (2008).
[42] V. Mateu, Phys. Rev. D **77**, 094020 (2008).
[43] Z.-H. Guo, O. Zhang, and H. Q. Zheng, AIP Conf. Proc. **1343**, 259 (2011).
[44] M. Luo, Y. Wang, and G. Zhu, Phys. Lett. B **649**, 162 (2007).
[45] J. J. Sanz-Cillero, D. L. Yao, and H. Q. Zheng, Eur. Phys. J. C **74**, 2763 (2014).
[46] M. Cleven, F.-K. Guo, C. Hanhart, and U.-G. Meißner, Eur. Phys. J. A **47**, 19 (2011).
[47] M.-L. Du, F.-K. Guo, and U.-G. Meißner, J. Phys. G (to be published).
[48] T. W. B. Kibble, Phys. Rev. **117**, 1159 (1960).
[49] B. Aubert *et al.* (*BABAR* Collaboration), Phys. Rev. Lett. **97**, 222001 (2006).
[50] J. Brodzicka *et al.* (Belle Collaboration), Phys. Rev. Lett. **100**, 092001 (2008).
[51] B. Aubert *et al.* (*BABAR* Collaboration), Phys. Rev. D **80**, 092003 (2009).
[52] M. F. M. Lutz and M. Soyeur, Nucl. Phys. **A813**, 14 (2008).
[53] K. A. Olive *et al.* (Particle Data Group), Chin. Phys. C **38**, 090001 (2014) and 2015 update.
[54] Z. H. Guo and J. J. Sanz-Cillero, Phys. Rev. D **79**, 096006 (2009).
[55] M. Jamin, J. A. Oller, and A. Pich, Nucl. Phys. **B622**, 279 (2002).
[56] Z. G. Wang, Eur. Phys. J. C **52**, 553 (2007).
[57] G. J. Ding, Phys. Rev. D **79**, 014001 (2009).
[58] W. A. Bardeen, E. J. Eichten, and C. T. Hill, Phys. Rev. D **68**, 054024 (2003).
[59] G. Ecker and C. Zauner, Eur. Phys. J. C **52**, 315 (2007).
[60] J. A. Oller and U.-G. Meißner, Phys. Lett. B **500**, 263 (2001).
[61] P. Buettiker and U.-G. Meißner, Nucl. Phys. **A668**, 97 (2000).
[62] M. Froissart, Phys. Rev. **123**, 1053 (1961).
[63] T. Hannah, Nucl. Phys. **B593**, 577 (2001).
[64] M. E. Bracco, M. Chiapparini, F. S. Navarra, and M. Nielsen, Prog. Part. Nucl. Phys. **67**, 1019 (2012).
[65] K. Azizi, Y. Sarac, and H. Sundu, Eur. Phys. J. C **74**, 3106 (2014).
[66] L. J. Reinders, H. Rubinstein, and S. Yazaki, Phys. Rep. **127**, 1 (1985).
[67] H. Y. Cheng, Y. Koike, and K. C. Yang, Phys. Rev. D **82**, 054019 (2010).
[68] G. L. Yu, Z. Y. Li, and Z. G. Wang, Eur. Phys. J. C **75**, 243 (2015).